Research Square

Preprints are preliminary reports that have not undergone peer review.
They should not be considered conclusive, used to inform clinical practice,
or referenced by the media as validated information.

Advanced Biochar Adsorbent via Catalyzed Microwave Pyrolysis for Targeted Herbicide Removal

Safa Waleed Shakir
University of Tikrit
Atheer M. Al-Yaqoobi
University of Baghdad
Saif Saleh Hussein
saifs.hussien@mtu.edu.iq

Middle Technical University

Research Article

Keywords: Biochar adsorption, Herbicide contamination, Microwave pyrolysis, Pinoxaden, Pseudo-second-order kinetics, Wastewater treatment

Posted Date: June 12th, 2026

DOI: https://doi.org/10.21203/rs.3.rs-9874789/v1

License: This work is licensed under a Creative Commons Attribution 4.0 International License.
Read Full License

Additional Declarations: No competing interests reported.

Advanced Biochar Adsorbent via Catalyzed Microwave Pyrolysis for Targeted Herbicide Removal

Safa W. Shakir[1], Atheer M. Al-Yaqoobi[2], Saif Saleh Hussein[3, *]

[1]Department of Chemical Engineering, College of Engineering, University of Tikrit, Tiktit, Iraq. Email: eng.safawaleed@tu.edu.iq, ORCID: 0000-0003-0621-9567

[2]Department of Chemical Engineering, College of Engineering, University of Baghdad, Baghdad, Iraq. Email: atheer.ghaleb@coeng.uobaghdad.edu.iq, ORCID: 0000-0001-9458-2723

[3]Technical College of Management-Baghdad, Middle Technical University, Baghdad, Iraq. Email: saifs.hussien@mtu.edu.iq, ORCID: https://orcid.org/0000-0003-0239-3517

[*]Corresponding author email: saifs.hussien@mtu.edu.iq

Abstract

The aim of the current study was the design of a sustainable and efficient adsorbent for pinoxaden removal, the recalcitrant herbicide increasingly found in aquatic environments through farm drainage. Chemical precipitation and biodegradation proved ineffectual for the removal of such contaminants, and thus there is a need for exploring biochar adsorption. Microwave pyrolysis of Dodonaea branch residues yielded biochar, which was post-tailored with MgO, $Ca_3(PO_4)_2$, and kaolinite for enhancing the physicochemical properties. The surface-modified biochar was investigated through BET surface area analysis, SEM, and FTIR. Maximum surface area (349 m^2/g), well-ordered meso-/micropores, and maximum number of oxygen-functional groups were for MgO-modified microwave-catalysed biochar (MC-Db), which showed superior adsorptive capacity. The experiments of adsorption were performed with diverse initial concentrations (5–85 mg/l), contact times (10–60 min), and adsorbent doses (0.25–2 g/l). The MgO-modified biochar exhibited the adsorptive capacity of the highest capacity of 119 mg/g for pinoxaden removal. The adsorption process followed the pseudo-second-order kinetics, whereas isotherm analysis showed an excellent fit with the Langmuir model, indicating monolayer adsorption over a uniform surface. The process spontaneity and exothermicity were validated through exploration of the study of the process of

thermodynamics. The results highlight the efficacy of the MgO-modified MC-Db as a low-cost and eco-friendly adsorbent with large capacity for application in the treatment of wastewater systems for the removal of herbicides. The study is a contribution towards the fast-emerging field of engineered biochar and highlights the need for surface modification through the assistance of catalysts for tailoring adsorptive applications. Future studies could be focused towards scale-up feasibility and regeneration performance for long-term application in the environment.

Keywords: Biochar adsorption; Herbicide contamination; Microwave pyrolysis; Pinoxaden; Pseudo-second-order kinetics; Wastewater treatment.

1. Introduction

Agricultural production has contributed to the high level of aquatic pollution due to the large use of agrochemicals [1]. Pinoxaden, a popular selective herbicide used in the production of cereal crops, has attracted a lot of special concern owing to its persistence and mobility in addition to the possibility of being toxic. Its tendency to seep into the waterways and ground water is also posing a risk to life and health of aquatic creatures and to humans, particularly in very agricultural areas [2, 3]. Pinoxaden may cause harm to aquatic life and alter aquatic ecosystems. It may also enter into the food chains of people by contaminated water or food products. The breakdown of herbicides like pinoxaden in water bodies presents a challenge to its destruction. The traditional remediation technologies, including chemical precipitation and microbial degradation are not applicable in the elimination of the stable and non-biodegradable compounds like pinoxaden. Thus, alternative methods to remediate herbicides should be explored which are less costly, sustainable, and highly effective [4].

Adsorption is a technology that has over the last ten years been successful and cost effective in the removal of organic pollutants in aquatic ecosystems. Adsorption refers to how the contaminant molecules adsorb to the surface of a solid adsorbent. This occurs through interactions such as hydrogen bonds, Van der Waals forces and electrostatic attraction [5, 6]. The use of biochar in adsorption processes are gaining more popularity, as they are economical, recyclable and environmentally friendly. Biochar is a porous carbon product generated by pyrolyzing biomass, and has had an enormous potential in the adsorption of pollutants [7, 8].

Its adsorptive capacity was however a limitation to their uses. The latest developments in the field of catalyst-supported microwave pyrolysis have provided a new opportunity to control the surface area, porosity and density of functional groups of the biochar. Pyrolysis is an edge technology to convert biomass to biochar, and it occurs in an anaerobic environment. When biochar is subjected to chemical and physical activation, it will alter its properties and become more effective in absorbing substances due to a larger surface area and the addition of functional groups such as carboxyl, carbonyl, and hydroxyl groups [9]. Different types of contaminants can be subjected to different types of interactions by functional groups, with successful adsorption processes. Biochar has also been utilized to assist in the removal of various types of pollutants in water including heavy metals, dyes and organic compounds by adsorbing them and purifying water [10]. Microwave pyrolysis is a new technology, which triggers the enhancement of the quality of biochar, bio-oil, and syngas due to the increase of heating rates [11-13]. Microwave heating technology has been demonstrated as an effective method of converting biomass to biochar and biofuels because it heats rapidly, uniformly and selectively and also because it is energy-efficient, inexpensive, and low maintenance since it uses portable equipment [14]. Hadiya (2022) experiments have validated the biochar as a common product of the microwave pyrolysis, and requires shorter time at steady-state temperatures than traditional pyrolysis [15]. Microwave pyrolysis has the potential to make biochar out of agricultural waste to be used in a variety of ways, such as carbon electrodes and magnetic biochar to purify wastewater. Biochar, condensate, and non-condensable gas are the main products of biomass pyrolysis, and their amounts depend on the final temperature and heating speed. Nevertheless, biomass is weakly microwave absorber [16, 17], and slow pyrolysis is caused by the microwave irradiation. Biomass may have additives, water, and ash to enable it to absorb microwave energy, potentially resulting in slow, intermediate, and rapid pyrolysis [13, 18]. Hence, the behaviour of biomass microwave-absorbing is the key determinant of output distribution of biomass pyrolysis. Despite biochar being a by-product of biomass pyrolysis, it can help augment the total incomes of processes. The weak absorption of microwave radiation in biomass materials is at times a problem that requires a microwave absorber to enhance the warming efficiency as is the case in pyrolysis. The most effective way to enhance the ultimate temperature of the biomass is by the use of catalysts during the reaction

of pyrolysis [19, 20]. Several catalysts, such as zeolite, metal oxides, metal carbonates, clays, and carbon-based substances, such as bentonite are applied in order to accelerate heating and increase production of bio-oil.

As time passes, however, its adsorption activity and capacity might decline, and hence require changes to improve its performance. With the addition of catalysts (e.g., alkali metals e.g., potassium hydroxide), acids (e.g., sulfuric acid), and metal salts (e.g., iron chloride), the adsorption capacity of the biochar was enhanced. The alteration has allowed it to acquire a greater surface area, more minute holes, and more active sites, which can assist it to react with harmful chemicals better [11,12]. Even catalyzed biochar demonstrated better kinetic and thermodynamic processes in adsorption, and to that end it can be a better instrument in the environmental remediation [21,22]. The mechanism by which the contaminants bind to the surfaces generally involves multiple stages, such as the binding of the contaminants to the surface, traveling through the pores on the biochar, and a period during which adsorption and desorption take place at a constant rate. Such processes will be analyzed by critically analyzing adsorption isotherms and kinetics. Such adsorption isotherms as Langmuir, Freundlich and Temkin will give significant information regarding the way the substances adsorb the surfaces, whether it occurs in a single layer or in many layers, and whether temperature and other factors influence this process [23]. Moreover, another approach used in adsorption, such as pseudo-first order, pseudo-second order, is significant as it provides data regarding the rate of substances sticking to surfaces, what determines the rate and how pinoxaden releases off the surfaces in water.

The present paper concentrates on the assist physicochemical characteristics of the microwave-catalyzed biochar (MC-Db) modification by three catalysts (MgO, Ca_3 $(PO_4)_2$ and Kaolinite) and is researching the adsorption capacity of the pinoxaden removal. the influence of contact time, adsorbate, and adsorbent concentration on the adsorption process Moreover, the isotherm models (Langmuir, Freundlich, pseudo-first order, pseudo-second order, and Temkin) were used to assess the behavior of adsorption and understand its properties. Significance of this study 0can provide a cost-effective, scalable and environmentally friendly technology to purify water contaminated with herbicides. This study does not just cover the issue of contaminated water but it also outlines the demands of the notion of a circular economy

and ecological waste disposal, namely, the valorization of agricultural waste and implementing energy-efficient microwave pyrolysis.

2. Methodology

2.1. Biomass processing

The Dedonea tree grows throughout Iraq. Dedonea branches (Db) were collected at Tikrit University College of Engineering. After trimming, the agricultural residual branches were carefully cleaned and oven-dried them at 60°C for 24 hours. Next, biomass was pulverized and sieved.

2.2. Preparing a biomass-catalyzed mixture

Microwave reactors were used for catalytic pyrolysis experiments. The reactor received 0.1 ml/min nitrogen. Before the experiment, Db was cleaned with deionized water, air-dried at 60°C for 24 hours, and sieved. Next, Db (2.5 mm) mixed with Kaolinite, MgO, and $Ca_3 (PO_4)_2$ catalysts. 20% wt. of catalysts mixed with Db participated in the experiments. Finally, the biomass and catalyst mixture underwent 15 min. of microwave-facilitated pyrolysis. After sieving, microwave-catalyzed biochar MC-Db was obtained. Procedures for experiments are shown in Fig. (1).

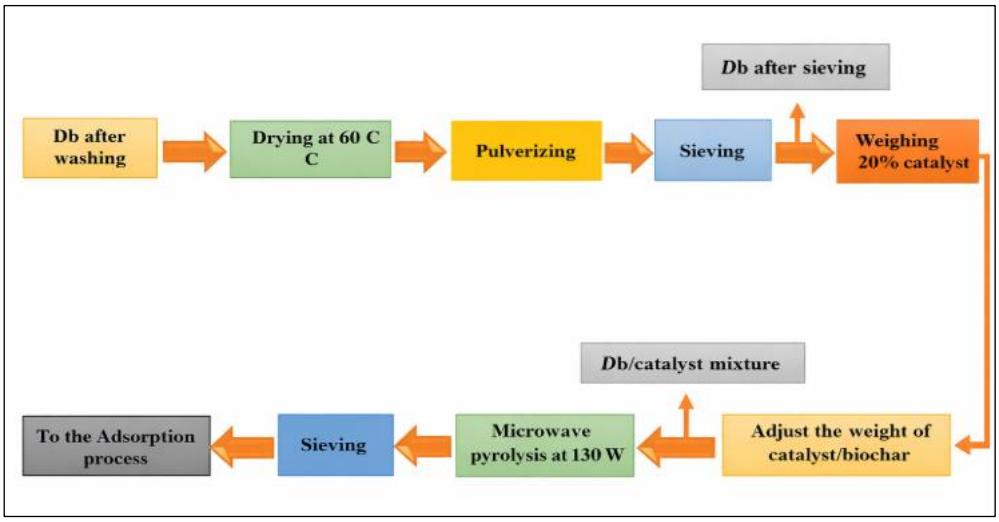


Figure 1. Preparation steps of MC-Db

2.3. Adsorption experiment

The adsorption experiments were conducted in a batch mode using a series of glass bottles containing 100 ml of pinoxaden solution at different initial concentrations of pinoxaden (5-35 mg/l), with adsorbent dosage of (0.5, 1, 1.5 and 2 g/l for (10–60 min.) and the equilibrium adsorption capacity measured after 24 hr to ensure the saturation capacity. The catalyzed biochar at a selected dose was added to the solution, and the mixture was shaken at 150 rpm for a specified contact time (10–60 minutes then to 24 hr.). The temperature of the solution was maintained at 25°C. After the adsorption experiment, the solution was filtered, and the concentration of pinoxaden was measured using high-performance liquid chromatography (HPLC) the adsorption process steps were conducted in Fig. 2.

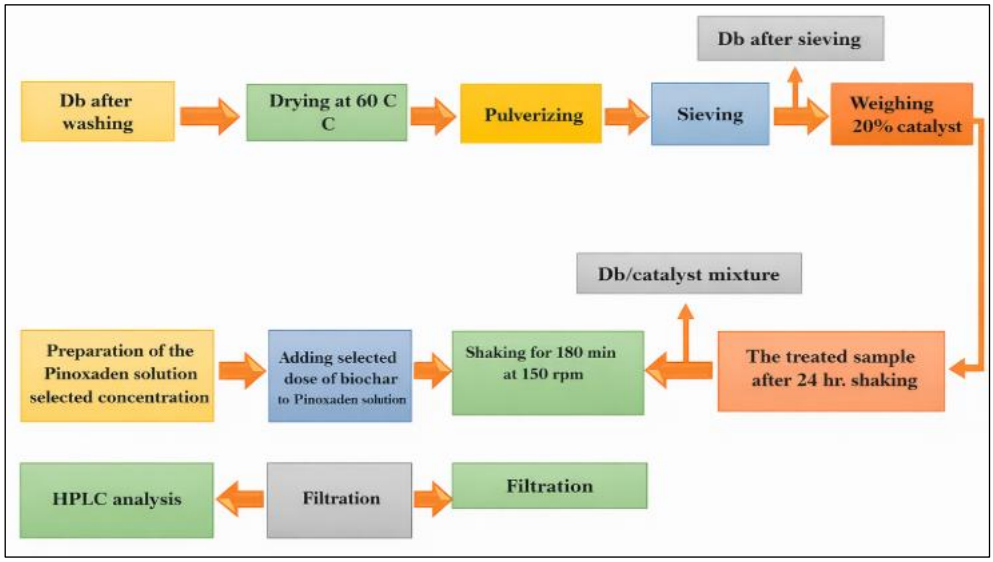


Figure 2 Adsorption experiment of pinoxaden

2.4. Measurement of adsorption capacity and the removal efficiency

The adsorption capacity and the removal efficiency of the MC-Db were calculated using Equ. (1) and (2) respectively [21]:

$$q = \frac{(C_0 - C_t) \times V}{m} \quad (1)$$

$$\text{eff.}\,\% = \frac{(C_0 - C_t)}{C_0} \times 100 \quad (2)$$

Where q is the adsorption capacity (mg/g), C_0 is the initial concentration of pinoxaden (mg/l), C_t is the concentration of pinoxaden at time t (mg/l), V is the volume of the solution (l) and m is the mass of the composite biochar (g).

The adsorption kinetics of biochar were evaluated using pseudo-first-order (Eq. (3)) and pseudo-second-order (Eq. (4)) kinetic models in order to elucidate the underlying adsorption mechanism [22].

$$\ln(q_e - q_t) = \ln q_e - k_1 t \quad (3)$$

$$\frac{t}{q_t} = \frac{1}{k_2 q_e^2} + \frac{t}{q_e} \quad (4)$$

Where q_e, q_t are adsorption capacity at equilibrium and at time t (mg/g), k_1 and k_2 are pseudo first and second order rates constants (min^{-1}) and t is time (min^{-1}).

The adsorption isotherm data of biochar were analysed using four models: the Langmuir (Eqs. 5 and 6), Freundlich (Eq. 7), and Temkin (Eq. 8) isotherms. The corresponding equations are presented as follows [23]:

$$q_e = \frac{q_{max} K_L C_e}{1 + K_L C_e} \quad (5)$$

$$R_L = \frac{1}{1 + K_L + C_i} \quad (6)$$

$$q_e = K_F C_e^{1/n} \quad (7)$$

$$q_e = Bln(K_T C_e) \quad (8)$$

Where:

q_e: Equilibrium adsorption capacity (mg/g).

C_e: Equilibrium concentration of adsorbate (mg/l).

q_{max}: Maximum monolayer adsorption capacity (mg/g).

K_L: Langmuir constant related to adsorption affinity (l/mg).

C_i: initial concentration (mg/l).

K_F: Freundlich constant indicating adsorption capacity ((mg/g)(l/mg)$^{1/n}$).

n: Heterogeneity factor (adsorption intensity).

K_T: Temkin equilibrium binding constant (l/mg).

$B = RT/b$: Temkin constant related to heat of adsorption (J/mol), R =8.314 J/mol.k, T= Absolute temperature (k), b: Temkin constant related to adsorption heat (J/mol).

2.5. Adsorbent characterization

A Scanning Electron Microscope (SEM) by MIRA III-Tescan (Czech) has provided energy-dispersive X-ray (EDX) and scanning electron microscope (SEM) analysis to determine the morphology, images and elemental composition of MC-Db. The images are captured at different magnifications (25×, 1000× and 4000×). The atomic and component percentages based on weight have been computed by the same SEM-EDX instrument. In order to investigate the elemental compositions, biomass materials have been examined without treating them. X-Ray Diffraction (PW1730 produced by Philips-Netherlands) has identified the X-ray diffraction (XRD) spectra with a 2θ scan range of 10 to 90 degrees. (Prep 060 and Gemini BET Machine) has carried out the (BET) analysis to calculate the surface area and a specific size of the biochar. Various methods have been used to obtain the measurements and the requisite functions or parameters (BET method, Langmuir method, t-method and BHJ method). The functional groups of biochar materials have been identified by Fourier transform infrared. PerkinElmer, Spectroscopy, FT-IR Spectrometer, Spectrum (2). The spectra are scanned with a phase

dimension of 1/cm and 8 scanning velocities that vary between wavenumbers 500 and 4000 1/cm.

3. Results and Discussion

3.1. MC-Db characterizations

3.1.1. Scanning electron microscopy (SEM)

One of the main methods used to study the surface morphology of biochar, including texture and porosity, and structural alterations such as pores and cracks which affect adsorption characteristics, is scanning electron microscopy (SEM). Fig. 3 (a,b and c) displays the SEM of Db and MC-Db using three kinds of catalyst.

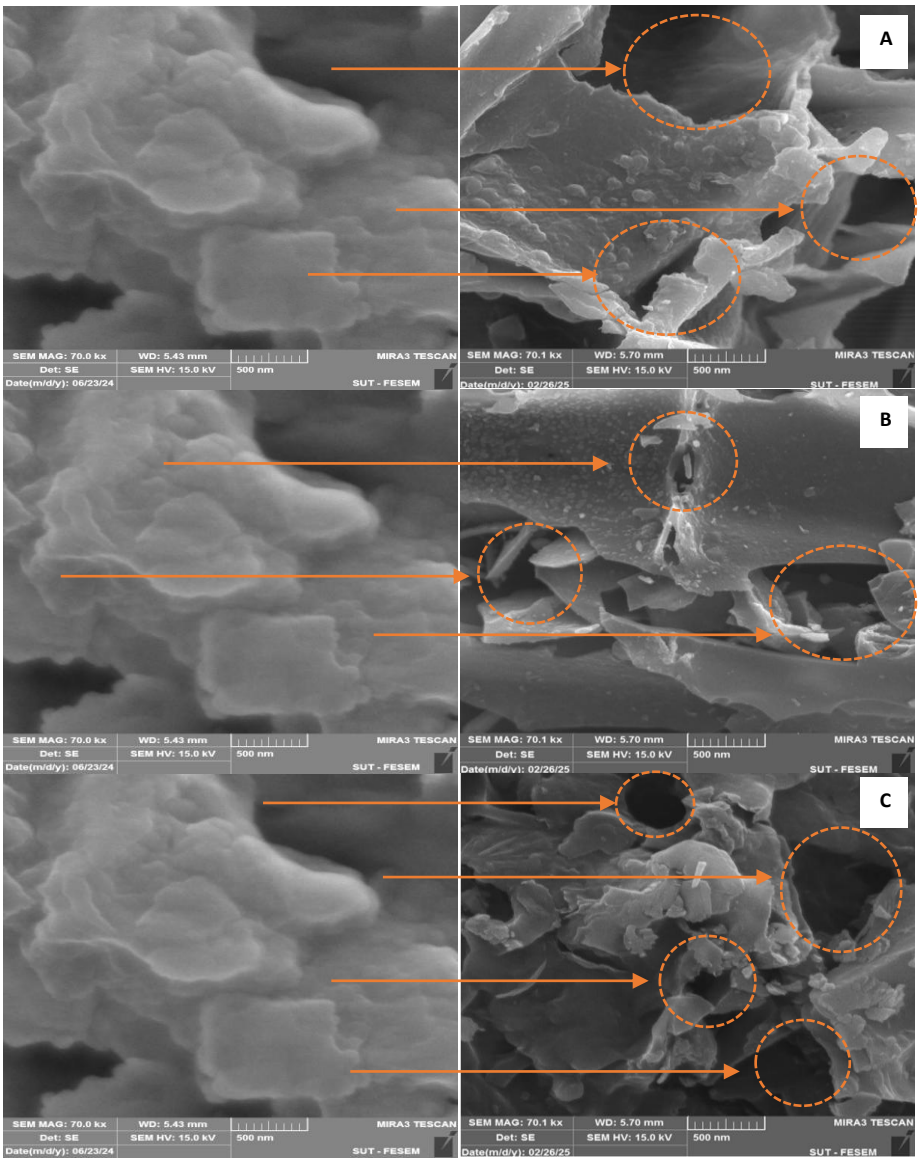


Figure 3. SEM of Db-130 W and MC-Db catalyzed with: a) $Ca_3(PO_4)$, b) Kaolinite and c) MgO

The SEM can also present high-resolution images, which can demonstrate basic morphological and textural information, including the location of the pores, the roughness of the surface, and structural alterations which might occur as a result of microwave exposure. The carbon deposit produced by the interactions of the volatile char could be the particulate matter. The destruction of the original fibrous structure of the Dedonea branches by the hot spot made MC-Db have a rougher and more fractured surface and enhanced the heating rate.

Following the pyrolysis process of catalysts, the attached bulky particles on the surface were more pronounced and blocked the pore channels. It was also found that there were mesoporous and micropore structures that had more regular ellipses. Fig. 3-a shows the effect of using $Ca_3(PO_4)_2$ as a catalyst. In line with this, it is apparent that when kaolinite is added as a catalyst, the surface morphology varies as shown in Fig. 3-b. We found new pores characterised by smooth roughness. Fig. 3-c, on the other hand, indicated that MC-Db that had MgO had an extremely rough surface with broken structures. One of the major influences of the application of MgO as the catalyst on the morphological transformation, i.e., the formation of the specific pores, as depicted by the red circles, on the surface roughness is evidently enhanced: the creation of the new cracks and channels.

Accordingly, the MgO had a very rough surface with fractured structures. It is possible to see mesoporous and microporous structures of more regular oval shapes. Moreover, the MC-Db are all characterised by a better surface morphology, which could be explained by the fact that the catalyst facilitates the formation of pores and structural change in the surface. This consequently influences the formation of "hot spots" by the pyrolysis process due to its direct influence on the heating process [24, 25].

3.1.2. Brunauer-Emmett-Teller (BET) analysis

Analysis is an important tool that helps in the definition of the adsorption capacity of microwave-catalysed biochar and optimising the production parameters to attain the desired surface properties to be used in environmental remediation. The MC-Db containing MgO exhibits the most surface area, 349 m^2/g, as shown in Table 1, and is likely to attain maximum adsorption of pinoxaden. On the other hand, kaolinite, a representative of clay minerals, has a moderate effect of 214 m^2/g compared to the addition of MgO. While MC-Db with $Ca3(PO_4)_2$ showed the lowest surface area of 145 m^2/g compared to the use of other catalysts. The available surface area of the biochar is determined by the BET surface area. The adsorptive sites of the MC-Db with a bigger surface area are more numerous. The contribution of the BET test to the pinoxaden adsorption process involves increased surface area and the existence of microporosity, which predisposes an excellent adsorptive potential [26]. Meso-porosity also promotes adsorption kinetics by enhancing faster diffusion. The reusability and optimality of

biochar in repeated adsorption cycles have been verified by the structural durability established by BET [27].

Table 1. BET analysis of the biochar with and without catalysts at 130 W for 20 min.

Sample	$S_{BET}(m^2/g)$	$V_p(cm^3/g)$	$r_P(nm)$
Biochar	3.0436	0.00812	13.21
Biochar+20% MgO	349.5	0.124	2.5
Biochar+20% $Ca_3(PO_4)_2$	145	0.47	5.2
Biochar+20% Kaolinite	214.8	0.311	3.7

3.1.3. Fourier-transform infrared spectroscopy (FTIR)

The Fourier-transform infrared spectroscopy of all MC-Db and Db-130W were shown in Fig. 4.

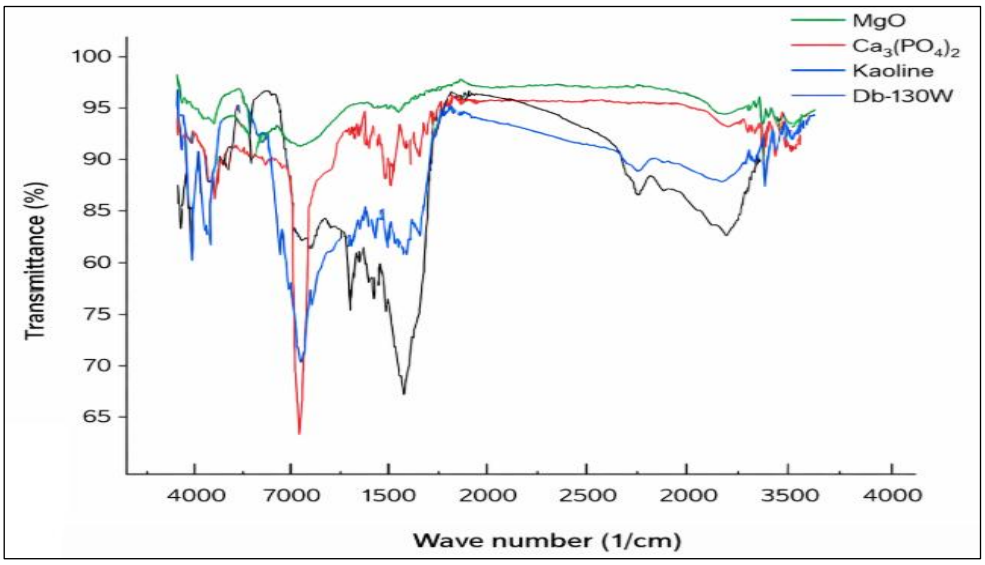


Figure 4. FTIR of all MC-Db and Db-130W

The presented FTIR spectrum displays the functional and structural group properties of: MC-Db samples with MgO, $Ca_3(PO_4)_2$, Kaoline, and the Db-130W. The black curve of the MgO

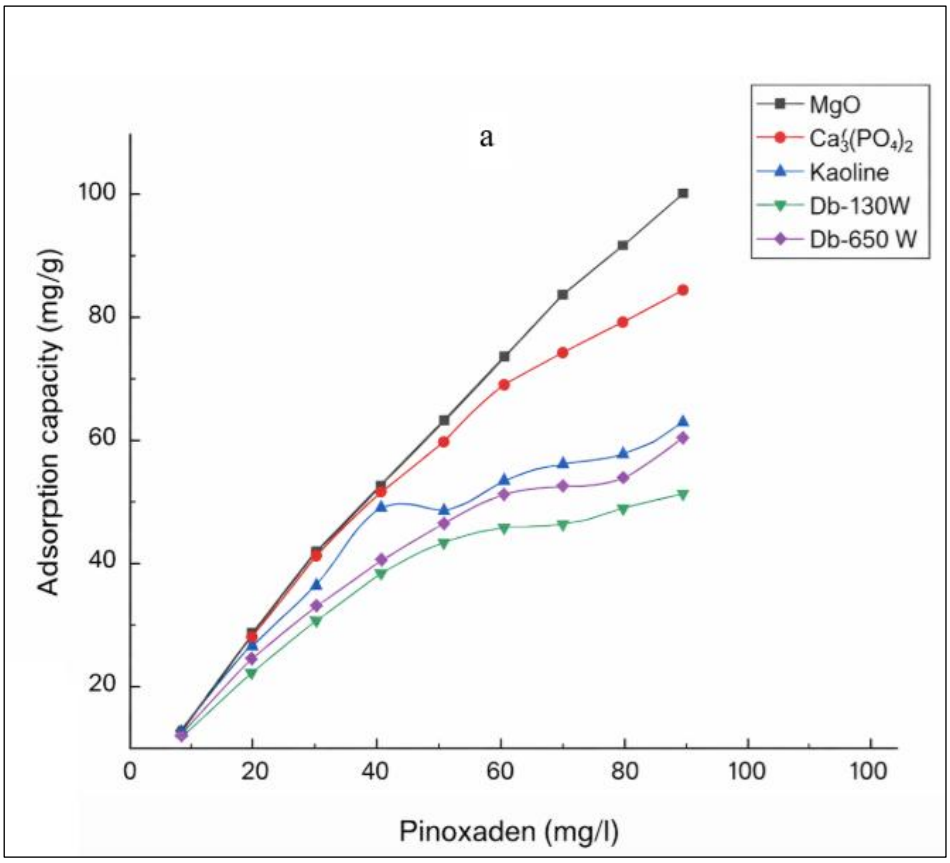
has intensive bands between 500–800 cm^{-1}, corresponding to stretching vibrations of the Mg–O bond, forming basic adsorption centers with the capability to strengthen the strength of electrostatic interaction with acid herbicides. Weak bands between 1400–1600 cm^{-1} can be attributed to the presence of carbonate groups, which can be part of the ion-exchange mechanism. The red curve of the $Ca_3(PO_4)_2$ includes intensive peaks at 1000–1100 cm^{-1}, corresponding to P–O asymmetric stretching vibrations in the phosphate groups, which are ligand-exchange and inner-sphere complexation active centers for herbicide molecules. PO_4^{3-} bending vibrations at 560–610 cm^{-1} further confirm this function, while a wide band of O–H stretching at 3400–3500 cm^{-1} corresponds to the presence of hydroxyl groups at the surface with the capability to form H bonds with polar functional groups of herbicides, increasing adsorption. Blue Kaolinite displays sharp, informative peaks at 3690–3620 cm^{-1} originating from inner and inner-surface hydroxyl stretching of Kaolinite responsible for polar surface and intensive hydrogen bonding. A broad O–H band corresponding to water around 3400 cm^{-1} and H–O–H bending around 1640 cm^{-1} suggest hydration at the surface, which is preferable for aqueous-phase interaction. Si–O stretching at 1000–1100 cm^{-1} provides π–π interaction site anchors or hydrogen bonds, whereas bands around 900 and below 600 cm^{-1} from Al–OH bending and Si–O–Al or Al–O–Si deformations can increase the reactivity at the surface and the cation exchange capacity. In contrast, the green series of Db-130W functionalized with the above materials, shows broader and smaller peaks characteristic of a heterogeneous and multifunctional surface. Broad bands at ~3400 cm^{-1} (O–H stretching) signify abundant hydroxyl groups for hydrogen interaction; ~2900 cm^{-1} (C–H stretching) for aliphatic groups for hydrophobic interaction with non-polar herbicides; and ~1600 cm^{-1} (H–O–H bending or C=C stretching) for aromatic regions for π–π electron donor–acceptor (EDA) interaction. Bands at 1000–1100 cm^{-1} signify C–O or residual Si–O bonding, which support surface complexation and hydrogen interaction. The composite feature of Db-130W integrates the functional benefits of the constituents to yield a multifunctional adsorbent with reactive spots available to engage in hydrogen interaction, electrostatic attraction, ion exchange, π–π interaction, and surface complexation. These cooperative processes significantly enhance its potential for effective adsorption of herbicides in the aqueous solution with low intensity [28,29].

3.2. Adsorption of pinoxaden

The adsorption of pinoxaden using three types of (MC-Db), Db130 and Db 650 W was investigated under different conditions, including initial concentration 5-85 mg/l), contact time (10-60 min.), and adsorbent concentration (0.25–2 g/l).

3.2.1. Pinoxaden initial concentration

The effect of initial concentration of pinoxaden (5–85 mg/l) on adsorption capacity and removal efficiency at dosage of MC-Db (0.5 g/l) for a time period of 60 minutes shown in Fig. 5 (a and b).



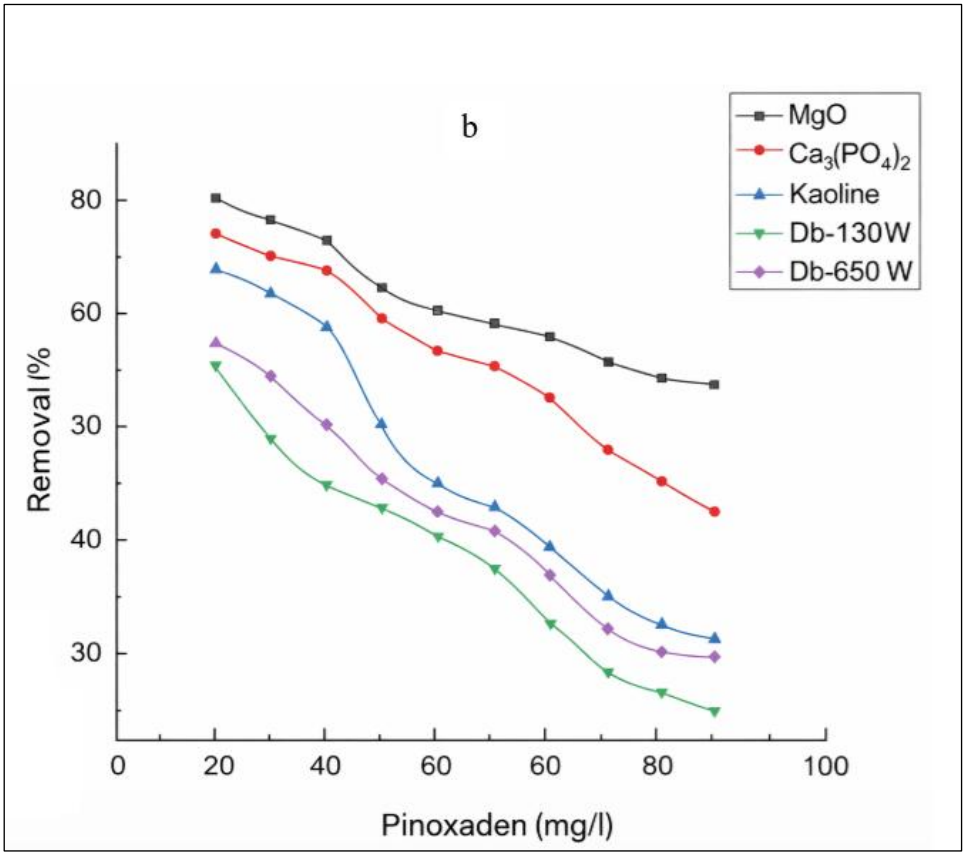


Figure 5. The influence of pinoxaden initial concentration on a) Adsorption capacity

b) Removal efficiency

Fig. 5a depicts how adsorption capacity rises with rising concentration, attaining a maximum value of about 110 mg/g when concentration is 85 mg/l for the case of MC-Db modified by MgO. Such a trend follows principles of adsorption, in which increased initial concentration provides greater force and more pinoxaden molecules for adsorption, enhancing the rate of collisions and diffusion towards active adsorption sites. The increased adsorption capacity of MgO-modified MC-Db is a result of increased surface area, enhanced porosity, and the formation of active chemically active sites consisting of Mg^{2+}, O^{2-}, and hydroxyl groups, favouring multiple adsorption mechanisms, including electrostatic attraction, hydrogen bonding, and surface complexation. Such an increment is synergistically generated to form chemisorptive bonds with active groups consisting of esters and heterocycles in pinoxaden,

boosting adsorption capacity to extraordinary dimensions [30-32]. $Ca_3(PO_4)_2$ modified MC-Db, for comparative purposes, demonstrated moderate adsorption (84 mg/g) by electrostatic attraction between the negatively charged molecule pinoxaden and accessible Ca^{2+} sites or protonated surfaces, while the performance of kaolinite-modified MC-Db demonstrated moderate performance (68 mg/g) on the basis of structural characteristics and modification [33, 34]. Other unmodified adsorbent biochars, Db-130W and Db-650W, demonstrated minimum adsorption (6.7–44 mg/g) with low surface area and pore volume, on the basis primarily of weaker physical modes of adsorption, which are reduced with saturation [35, 36]. As expected, adsorption capacity increased when pinoxaden concentration increased up to surface saturation, a point by which adsorption is not feasible [35, 36].

Conversely, as seen from Fig. 5-b, removal efficiency reduced with rising concentration in all the adsorbent materials—from 67 to 34% in Db-130W, from 70 to 37.6% in Db-650W, from 80.4 to 49% in MgO–MC-Db, from 80 to 49% in $Ca_3(PO_4)_2$–MC-Db, and from 77 to 40% in Kaolinite–MC-Db—due to the lesser number of adsorption sites becoming filled with rising concentration. There are abundant sites at low concentrations, with maximum removal efficiency, whereas more competition for the limiting sites with rising amounts of pinoxaden results in a smaller percentage of contaminant removed from solution, a fact corroborated by earlier studies [37, 38].

3.2.2. The influence of contact time

Fig. 6 (a and b) illustrate the adsorption capacity (mg/g) and pinoxaden removal efficiency against contact time (10–60 minutes) for unmodified and various modified microwave-catalysed biochar (MC-Db).

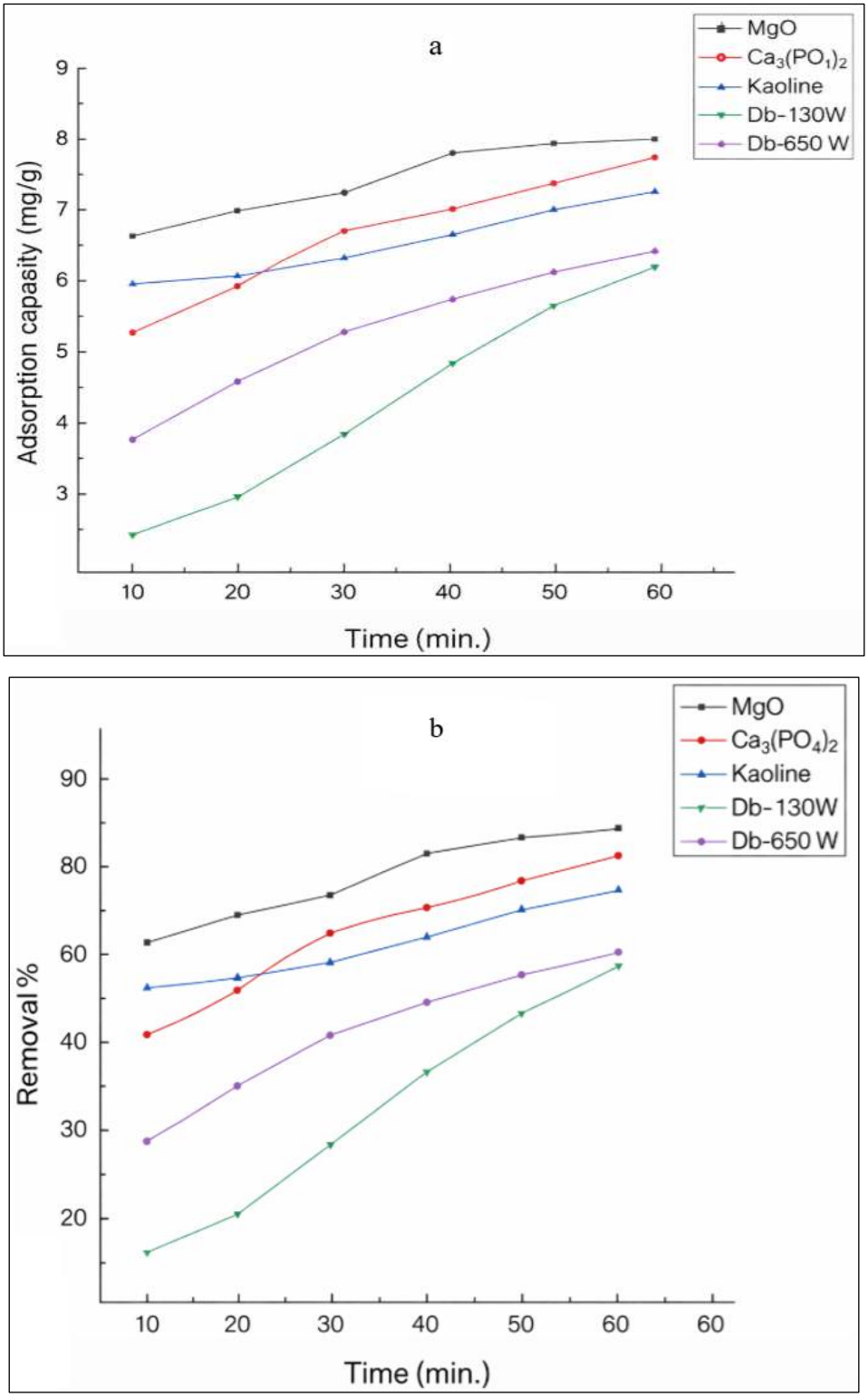


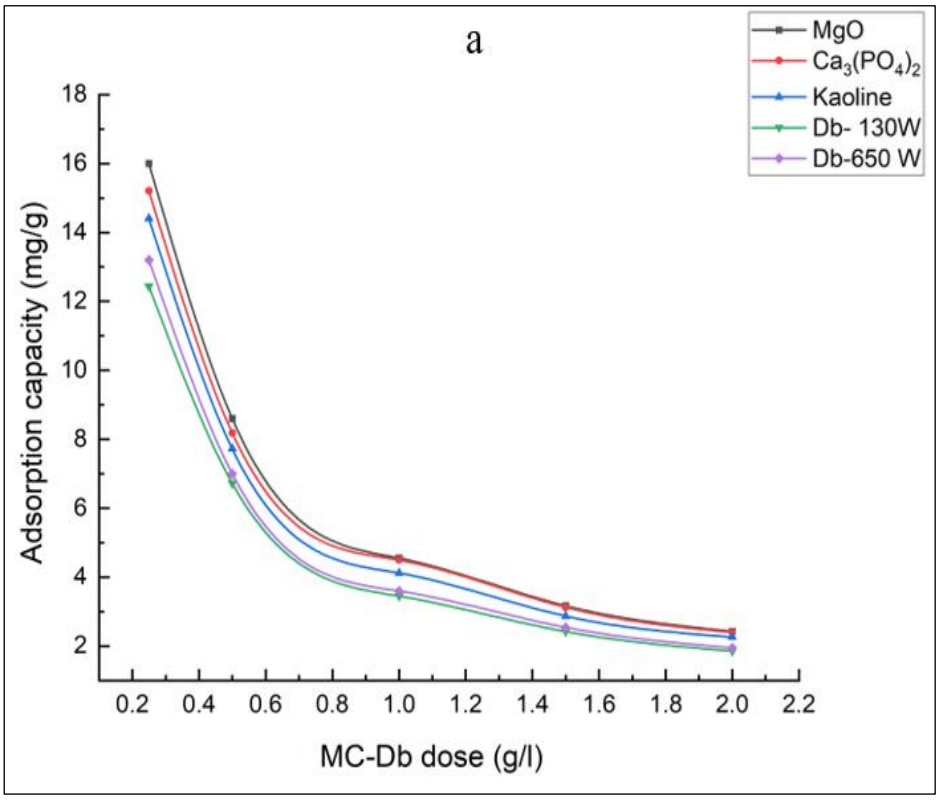
Figure 6. The influence of contact time of adsorption of pinoxaden at 5 mg/l and dosage of 0.5 g/l on a) Adsorption capacity b) Removal efficiency

At an initial pinoxaden concentration of 0.5 mg/l and adsorbent dosage of 0.5 g/l. As is evident, the adsorption capacity and removal efficiency are quite high in the initial 10–40 minutes, which is most probably due to a large number of active sites on the adsorbents facilitating the rapid adsorption of pinoxaden molecules. As the contact time is extended beyond 40 minutes, the adsorption rate becomes sluggish and eventually reaches equilibrium at 60 minutes, indicating that most active sites are filled and the system is saturated [39, 40]. Among the adsorbent samples, MgO-modified MC-Db demonstrated maximum adsorption capacity, which is enhanced from approximately 6.9 mg/g at 10 minutes to approximately 8.6 mg/g at 60 minutes, thanks to its enhanced surface area, porosity, and reactive Mg^{2+} sites facilitating rapid and strong chemisorptive adsorption with pinoxaden. MC-Db modified with $Ca_3(PO_4)_2$ also demonstrated appreciable adsorption from ~5.8 to ~8 mg/g, since it may be enhanced by electrostatic attraction with phosphate groups and herbicide. Similarly, kaolinite-modified MC-Db also demonstrated a steady increasing trend from ~6 to ~7.7 mg/g, albeit with slower kinetics through fewer reactive sites and differences in surface chemistry. Conversely, unmodified biochar Db-130W and Db-650W recorded the lowest performances, from ~3 to ~6.7 mg/g and ~4.5 to ~7 mg/g, respectively, through limited surface area and porosity, facilitating slow and poor physical adsorption. These findings underscore the superiority of MgO–MC-Db and the catalyst-supplemented biochar, which not only displayed the greatest adsorption but also the most rapid kinetics and reached equilibrium in a mere 60 minutes. The overall profile of adsorption, a rapid initial uptake followed by levelling off, is consistent with a chemisorption mechanism exhibiting pseudo-second-order kinetics and distinguishes a fast and effective adsorption process suitable for application. The figure depicts the removal efficiency of pinoxaden from 10 to 60 minutes by various modified and unmodified microwave-catalysed biochar (MC-Db), showing the role of surface modification. Maximum efficiency (70–85)% was achieved by MgO-modified biochar due to its high surface area and basic sites for strong chemisorption. It was followed by $Ca_3(PO_4)_2$-modified biochar (65–78)%, promoted by phosphate and calcium sites. Kaolinite-modified biochar showed moderate performance (62–74)% due to improved structure. On the contrary, raw biochar (Db-130W and Db-650W) showed lower efficiencies (48–68)% and (42–64)% due to low surface activity. All adsorbents

showed rapid adsorption within the first 40 minutes, followed by a plateau as active sites became saturated, which is a characteristic of typical chemisorption.

3.2.3. The influence of MC-Db dosage

The impact of MC-Db dosage (0.25-2 g/l) on the adsorption capacity and removal efficiency of pinoxaden at 0.5 mg/l for 60 min. is illustrated in Fig. 7 (a and b).



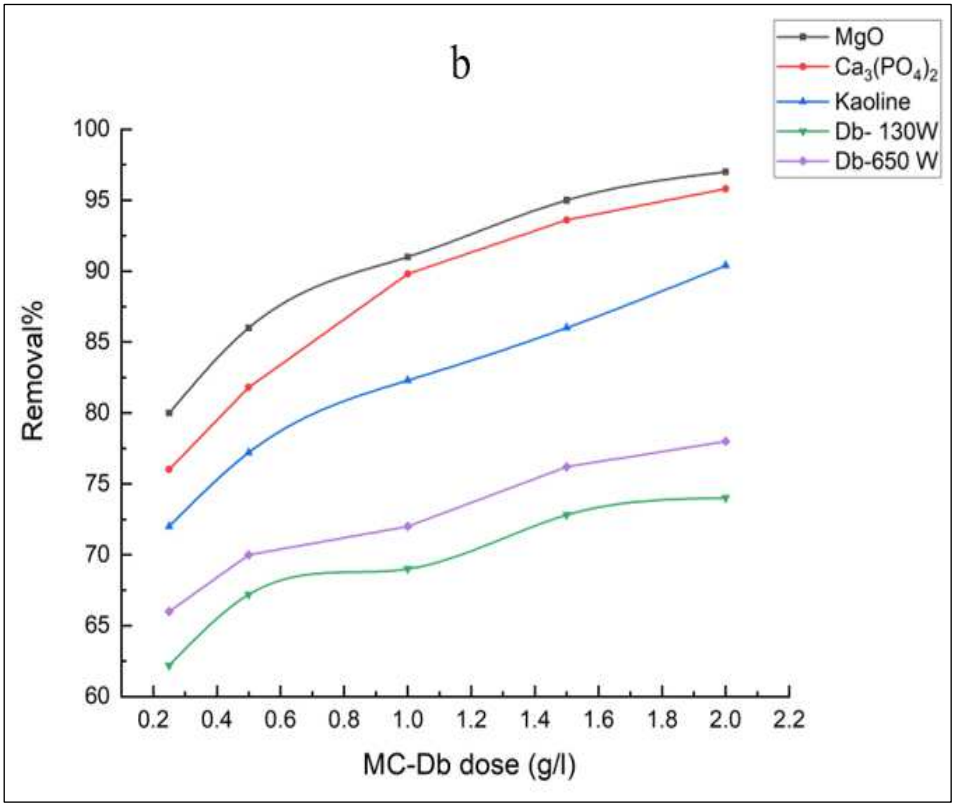


Figure 7. The impact of MC-Db dosage at 5 mg/l of pinoxaden a) Adsorption capacity

b) Removal Efficiency

The plot reflects the inverse relationship between adsorbent dosage and adsorption capacity (mg/g) of pinoxaden by various microwave-catalysed biochars (MC-Db), modified (MgO, $Ca_3(PO_4)_2$, and kaolinite) and unmodified (Db-130W and Db-650W), over a range of 0.25-2.0 g/l. At low dosages, particularly 0.2 g/l, the MgO-modified MC-Db exhibited the highest adsorption capacity 15.8 mg/g, followed by $Ca_3(PO_4)_2$ 14.68 mg/g and kaolinite-modified (4.4 mg/g, with lower-performing unmodified (Db-130W, Db-650W) at 13.2 and 12.44, respectively. Higher adsorption at low dosages is attributed to greater surface area, high density of reactive surfaces, and better surface chemistry within the modified biochar in enhancing effective adsorption of pinoxaden [39, 40]. However, at greater dosages, adsorption capacity slowly tapers off across all adsorbents, falling below 3 mg/g at 2.0 g/l. This is due to a greater constant concentration of pinoxaden being dispersed over a greater adsorbent mass, leading to reduced ratios between adsorbents and pollutants, with potential agglomerations between particles diminishing accessible surface areas [41, 42]. As greater dosages provide decreasing

adsorption capacity on a gram basis, they can still provide enhanced total removal efficiency, demonstrating a compromise between total removal capacity and cost-performance. These results are characteristic of regular adsorption behavior and reflect optimization between adsorbent dosage within practical applications for a compromise between effectiveness and cost.

Fig. 7-b illustrates the effect of different doses (0.2 to 2.0 g/l) of MC-Db, Db-130W, and Db-650W on pinoxaden removal performance. Dose-dependent removal performance enhancement can be seen across all the materials, suggesting the key role regarding adsorbent dosage for contaminant adsorption optimisation. Among all the samples tested, MgO-modified biochar showed the best removal performance, reaching about 98% at its highest dose, followed closely by $Ca_3(PO_4)_2$ and kaolinite composites, which also performed very well. Nonmodified biochar (Db-130W as well as Db-650W), on the other hand, had comparatively low removal performances, with plateaus at 75% as well as 72%, with signs of limited adsorptive performance as a result of possibly low surface reactivity as well as lack of benefit from functionalisation. MgO as well as $Ca_3(PO_4)_2$, composite's superior performance is due to higher surface area and higher basicity, as well as surface-reactive functional groups, making it higher in interaction with contaminants [43]. These findings show surface functionalisation as well as dosage optimisation as driving forces for full adsorption performance, as is consistent with recent studies focusing on functionalised material as well as specific operating parameters' necessity for effective treatment of waters as well as wastewaters [28, 44].

3.3. Adsorption Isotherms

The adsorption isotherm data are presented in Figures 8–10 and also summarized in Table 2.

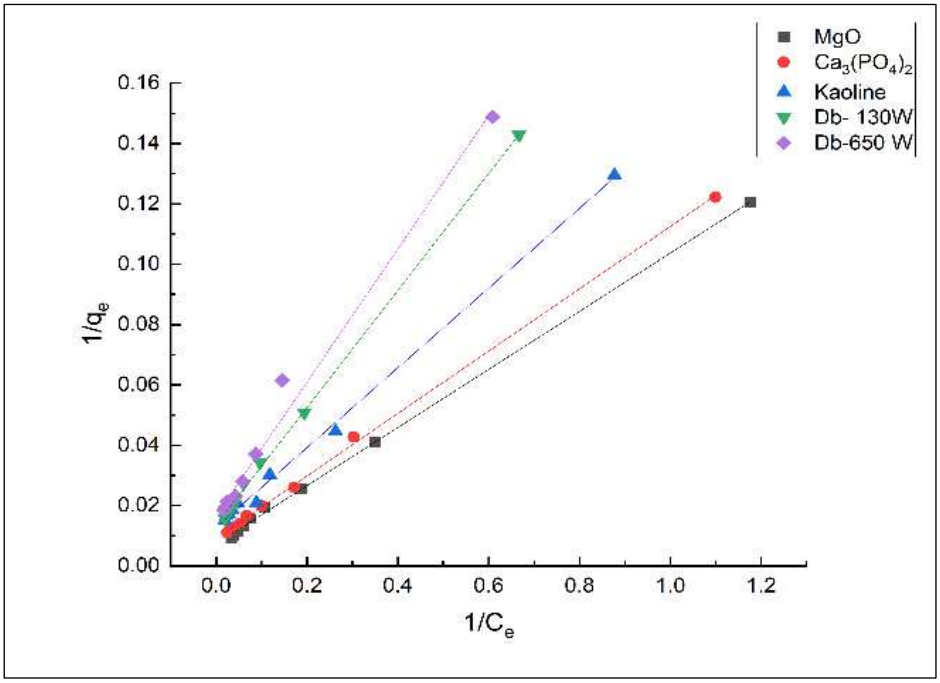


Figure 8. Langmuir model for all MC-Db

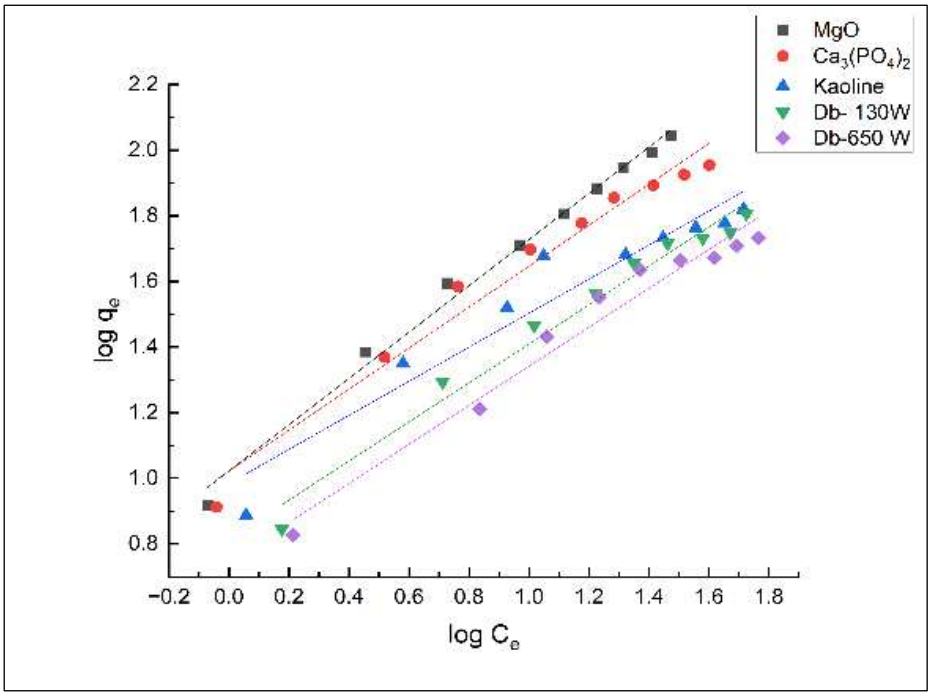


Figure 9. Freundlich model for all MC-Db

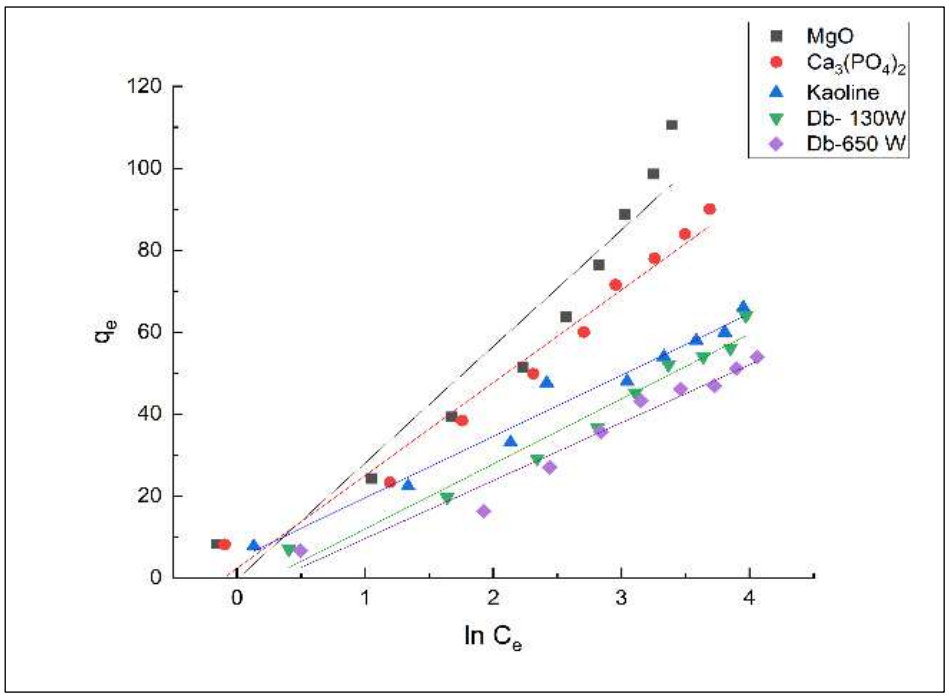


Figure 10. Temkin model for all MC-Db

Table 2 The isotherm of all MC-Db and biochar.

MC-Db	Langmuir			Freundlich				Temkin		
	K_L	q_{max}	R^2	R_L	n	R^2	$Log\ K_F$	B	K_T	R^2
Db 130W	0.068	59.88	0.984	0.725	1.369	0.954	0.626	12.53	0.86	0.934
+20% MgO	0.075	137.55	0.999	0.69	1.41	0.99	1.022	28.42	0.989	0.9089
+20% $Ca_3(PO_4)_2$	0.093	103.84	0.999	0.68	1.64	0.956	1.023	21.8	1.17	0.968
+20% Kaolinite	0.096	78.12	0.996	0.656	1.98	0.908	0.984	14.34	1.388	0.934
Db 650W	0.07	73.2	0.998	0.739	1.68	0.97	0.815	15.85	0.783	0.963

That reveals insightful differences among the modified and unmodified microwave-catalysed biochar MC-Db, highlighting the impact of catalyst type on the removal of pinoxaden.

Isotherm parameters for various MC-Db best fit Langmuir and Freundlich as well as Temkin model equations, detailing adsorption mechanisms of pinoxaden. The Langmuir model best explained all samples, particularly MgO- as well as $Ca_3(PO_4)_2$-modified MC-Db, with R^2=0.999, i.e., monolayer adsorption on a homogeneous surface with a limited number of equivalent high-energy sites. MgO-modified MC-Db had the highest adsorption capacity q_{max}=137.55 mg/g, followed by $Ca_3(PO_4)_2$-modified q_{max}=103.84 mg/g due to enhanced surface area, basic nature, and availability of reactive functional groups or ions for strong chemisorptive interactions, including electrostatic attraction as well as surface complexation with acidic pinoxaden molecules [43, 44]. Kaolinite-modified MC-Db, despite being high performing q_{max}=78.12 mg/g, had relatively low adsorption performance, possibly due to reduced functional diversity as well as moderate reactivity. Db-130W as well as Db-650W, being nonmodified biochar, had low q_{max} 59.88 as well as 73.2 mg/g values, i.e., limited surface functionality as well as a low number of active sites. Though the Freundlich model, assuming heterogeneous adsorption sites, gave reasonable n values (>1), its low R^2 values suggest it to be a poorer-fitting model than Langmuir in describing the prevailing mechanism. The Temkin model also attests to this chemisorption nature, as greater Bt as well as K_T values in MgO and $Ca_3(PO_4)_2$ samples indicate strong adsorbate-adsorbent interactions. Referred Langmuir-type adsorption confirms such a saturation behaviour: after one active site gets filled, no subsequent adsorption on it takes place, which is necessary for the optimised dosage of adsorbent as well as designing effective water treatment systems [28, 45]. Overall, these findings emphasise how surface modification improves adsorption performance through the generation of surface-activated, homogeneous sites, consistent with recent trends in new adsorbent development.

3.4. Adsorption kinetics

Pinoxaden adsorption kinetics over MC-Db biochar is presented in Table 3, where both pseudo-first-order and pseudo-second-order kinetic equations were employed to examine the adsorption mechanism.

Table 3. Dynamics parameters for pinoxaden adsorption into MC-Db.

MC-Db	Pseudo-first-order			Pseudo-second-order		
	q_e	K_1	R_1	q_e	K_2	R_2
Db 130W	2.69986	-0.08522	0.70186	9.914733	0.003072	0.86599
MgO-Db	5.528961	-0.05847	0.9481	7.784524	0.014817	0.99683
Ca3(PO4)2-Db	4.212263	-0.0355	0.956	8.756567	0.016744	0.9941
Kaolinite-Db	3.064854	-0.0459	0.8114	7.961783	0.029991	0.9932
Db 650W	5.53	-0.0584	0.948	7.78	0.0148	0.996

The kinetics modelling result of this study reveals pinoxaden adsorption on various types of biochar is best described by the pseudo-second-order rather than the pseudo-first-order model, confirming chemisorption as the dominant mechanism. Among all modified biochar, MgO-Db exhibited the maximum rate constant for kinetics K_2=0.03 g/mg·min and a high correlation value R^2=0.99, confirming a high rate and efficiency in adsorption due to augmented surface activity and porosity due to MgO. The minimum rate constant confirms even with the maximum q_e=8.75 mg/g at equilibrium, $Ca_3(PO_4)_2$-Db exhibited reduced kinetics. Kaolinite-Db also exhibited maximum rate fit and decent adsorption capacity, harmonising speed and efficiency. The findings are corroborated by other studies, such as the adsorption process on corn cob biochar prepared under various pyrolysis conditions, whereby pseudo-second-order best fit is described, indicative of chemisorption as the dominant mechanism [46-49]. In a similar setup, higher removal of paraquat from water-contaminated samples by cell-immobilised biochar conformed to pseudo-second-order kinetics, confirming a role played by chemisorption [50-53]. These comparisons verify how efficient biochar is, particularly when it is modified or prepared under desired conditions, in removing recalcitrant organic pollutants such as pinoxaden from water.

3. Conclusions

This study highlights the potential of composite biochar as a sustainable and effective adsorbent for the removal of pinoxaden from wastewater. The results indicate that the catalytic modification of microwave-assisted biochar, MC-Db, with MgO, $Ca_3(PO_4)_2$, and kaolinite

considerably changed the materials' physicochemical properties, mostly their surface area, porosity, and active functional groups, all of which are fundamental to their adsorptive effectiveness. Of the three, the most pronounced enhancement was with MgO-modified biochar, with 349 m^2/g for BET surface area, as compared with 214 m^2/g for kaolinite and 145 m^2/g for $Ca_3(PO_4)_2$ modification. This is explainable by the catalytic effect of MgO in favor of devolatilization and pore development in microwave pyrolysis, promoting the formation of highly developed meso- and microporous structures. Total pore volume and mean pore size were also greater for MgO-Db, demonstrating greater porosity construed as beneficial for the diffusion and access of the herbicide molecules into the pores. On the surface chemistry aspect, FTIR analysis and Boehm titration confirmed the reality that the surface of MgO-Db contained the highest number of oxygen-bearing functionalities such as hydroxyl, carbonyl, and carboxyl groups, which are responsible for electrostatic interaction and hydrogen bonding with the polar contaminant pinoxaden. All these structural and chemical differences are the reasons for the superiority of the MgO-Db over the others in the capacity for adsorption, offering with it a more porous structure with a richer chemistry for the sequestration of the herbicide.

Acknowledgment

The authors would like to express their sincere gratitude to Tikrit University, Baghdad University and Middle Technical University, for their continuous support, valuable guidance, and for providing the necessary academic environment and facilities that contributed to the successful completion of this research work.

Conflicts of Interest

The authors declare that there is no conflict of interest regarding the publication of this paper. The authors confirm that they have no known competing financial interests or personal relationships that could have influenced the work reported in this study.

Funding sources

The authors declare that no funding was received for the conduct of this study.

Author Contributions

Safa Waleed Shakir conceptualized and developed the initial research idea. **Atheer M. Al-Yaqoobi** supervised the overall data collection process. **Saif Saleh Hussein** was responsible for the investigation and methodology.

References

[1] AbuQamar SF, El-Saadony, M. T., Alkafaas, S. S., Elsalahaty, M. I., Elkafas, S. S., Mathew, B. T, & El-Tarabily, K A. Ecological impacts and management strategies of pesticide pollution on aquatic life and human beings. *Marine Pollution Bulletin* 2024; 206: 116613. https://doi.org/10.1016/j.marpolbul.2024.116613

[2] Kumar R, Sankhla MS, Kumar R, Sonone SS. Impact of pesticide toxicity in aquatic environment. *Biointerface Research in Applied Chemistry* 2021; 11(3): 10131–10140. https://ssrn.com/abstract=3755402

[3] Shakir SW, Hussein SS, Khazaal SH, Al-Naseri HA, Ahmed AM, Hachim RN, Al-Dahhan MH. Examination and improvement of the Taguchi-based nanofluids impact on CO_2 absorption using Al_2O_3 nanoparticles. *Journal of Advanced Research in Fluid Mechanics and Thermal Sciences* 2024; 120(1): 204–216. https://doi.org/10.37934/arfmts.120.1.204216

[4] Larramendy ML, Soloneski S, editors. *Pesticides: Updates on Toxicity, Efficacy and Risk Assessment*. BoD–Books on Demand; 2022. 326 pp.

[5] Abbas AS, Ahmed MJ, Darweesh TM. Adsorption of fluoroquinolones antibiotics on activated carbon by K_2CO_3 with microwave assisted activation. *Iraqi Journal of Chemical and Petroleum Engineering* 2016; 17(2): 15–23. https://doi.org/10.31699/IJCPE.2016.2.3

[6] Jawad SSM, Khalaf ZA, Shakir SW. Extracting oil from oil shale using internal distillation (in situ retorting). *Open Engineering* 2023; 13(1): 20220460. https://doi.org/10.1515/eng-2022-0460

[7] Siipola V, Pflugmacher S, Romar H, Wendling L, Koukkari P. Low-cost biochar adsorbents for water purification including microplastics removal. *Applied Sciences* 2020; 10(3): 788. https://doi.org/10.3390/app10030788

[8] Sadegh F, Sadegh N, Wongniramaikul W, Apiratikul R, Choodum A. Adsorption of volatile organic compounds on biochar: A review. *Process Safety and Environmental Protection* 2024; 182: 559–578. https://doi.org/10.1016/j.psep.2023.11.071

[9] Paikamnam A, Clowutimon W, Chanpee S, Sriprom P, Assawasaengrat P. Production of empty palm bunch biochar using microwave-assisted pyrolysis at low temperature. *AIP Conference Proceedings* 2021; 2397(1). https://doi.org/10.1063/5.0064053

[10] Qiu B, Shao Q, Shi J, Yang C, Chu H. Application of biochar for the adsorption of organic pollutants from wastewater: Modification strategies, mechanisms and challenges. *Separation and Purification Technology* 2022; 300: 121925. https://doi.org/10.1016/j.seppur.2022.121925

[11] Abd MF, Al-Yaqoobi AM. The feasibility of utilizing microwave-assisted pyrolysis for Albizia branches biomass conversion into biofuel productions. *International Journal of Renewable Energy Development* 2023; 12(6): 1061–1069. https://doi.org/10.14710/ijred.2023.56907

[12] Abd MF, Al-Yaqoobi AM. The potential significance of microwave-assisted catalytic pyrolysis for valuable bio-products driven from Albizia tree. *Applied Science and Engineering Progress* 2025; 18(1): 7454–7454. https://doi.org/10.14416/j.asep.2024.07.016

[13] Abd MF, Al-Yaqoobi AM, Abdul-Majeed WS. Catalytic microwave pyrolysis of Albizia branches using Iraqi bentonite clays. *Iraqi Journal of Chemical and Petroleum Engineering* 2024; 25(2): 175–186. https://doi.org/10.31699/IJCPE.2024.2.16

[14] Qiu T, Li C, Guang M, Zhang Y. Porous carbon material production from microwave-assisted pyrolysis of peanut shell. *Carbon Research* 2023; 2(1): 45. https://doi.org/10.1007/s44246-023-00079-9

[15] Hadiya V, Popat K, Vyas S, Varjani S, Vithanage M, Gupta VK, Patel Z. Biochar production with amelioration of microwave-assisted pyrolysis: Current scenario, drawbacks and perspectives. *Bioresource Technology* 2022; 355: 127303. https://doi.org/10.1016/j.biortech.2022.127303

[16] Behera S, Samal K. Sustainable approach to manage solid waste through biochar assisted composting. *Energy Nexus* 2022; 7: 100121. https://doi.org/10.1016/j.nexus.2022.10012

[17] Mahmood SS, Al-Yaqoobi AM. Microwave assisted production of biodiesel using CaO nano-catalyst produced from mango fallen leaves extract. *Journal of Ecological Engineering* 2025; 26(1). https://doi.org/10.12911/22998993/195650

[18] Shi K, Yan J, Menéndez JA, Luo X, Yang G, Chen Y, Wu T. Production of H_2-rich syngas from lignocellulosic biomass using microwave-assisted pyrolysis coupled with activated carbon enabled reforming. *Frontiers in Chemistry* 2020; 8: 3. https://doi.org/10.3389/fchem.2020.00003

[19] Foong SY, Liew RK, Yang Y, Cheng YW, Yek PNY, Mahari WAW, Lam SS. Valorization of biomass waste to engineered activated biochar by microwave pyrolysis: Progress, challenges, and future directions. *Chemical Engineering Journal* 2020; 389: 124401. https://doi.org/10.1016/j.cej.2020.124401

[20] Ren X, Ghazani MS, Zhu H, Ao W, Zhang H, Moreside E, Bi X. Challenges and opportunities in microwave-assisted catalytic pyrolysis of biomass: A review. *Applied Energy* 2022; 315: 118970. https://doi.org/10.1016/j.apenergy.2022.118970

[21] Doble J, Wilson G, Wainman JW. Kinetic and thermodynamic analysis of the adsorption of methylene blue onto biochar. *Journal of Chemical Education* 2023; 100(10): 4040–4046. https://doi.org/10.1021/acs.jchemed.3c00518

[22] Lingamdinne LP, Angaru GKR, Pal CA, Koduru JR, Karri RR, Mubarak NM, Chang YY. Insights into kinetics, thermodynamics, and mechanisms of chemically activated sunflower stem biochar for removal of phenol and bisphenol-A from wastewater. *Scientific Reports* 2024; 14(1): 4267. https://doi.org/10.1038/s41598-024-54907-y

[23] Shikuku VO, Mishra T. Adsorption isotherm modeling for methylene blue removal onto magnetic kaolinite clay: A comparison of two-parameter isotherms. *Applied Water Science* 2021; 11(6): 103. https://doi.org/10.1007/s13201-021-01440-2

[24] Ke L, Zhou N, Wu Q, Zeng Y, Tian X, Zhang J, Wang Y. Microwave catalytic pyrolysis of biomass: A review focusing on absorbents and catalysts. *npj Materials Sustainability* 2024; 2(1): 24. https://doi.org/10.1038/s44296-024-00027-7

[25] Qiu L, Li C, Zhang S, Wang S, Li B, Cui Z, Hu X. Importance of oxygen-containing functionalities and pore structures of biochar in catalyzing pyrolysis of homologous poplar. *Chinese Journal of Chemical Engineering* 2024; 65: 200–211. https://doi.org/10.1016/j.cjche.2023.09.002

[26] Zou J, Fan C, Jiang Y, Liu X, Zhou W, Xu H, Huang L. A preliminary study on assessing the Brunauer-Emmett-Teller analysis for disordered carbonaceous materials. *Microporous and Mesoporous Materials* 2021; 327: 111411. https://doi.org/10.1016/j.micromeso.2021.111411

[27] Potnuri R, Rao CS. Synthesis and characterization of biochar obtained from microwave-assisted copyrolysis of torrefied sawdust and polystyrene. *ACS Sustainable Resource Management* 2024; 1(9): 2074–2085. https://pubs.acs.org/doi/10.1021/acssusresmgt.4c00195

[28] Zhang Y, Fan S, Liu T, Fu W, Li B. A review of biochar prepared by microwave-assisted pyrolysis of organic wastes. *Sustainable Energy Technologies and Assessments* 2022; 50: 101873. https://doi.org/10.1016/j.seta.2021.101873

[29] Shakir SW, Al-Yaqoobi AM. Parametric and characteristic evaluation of microwave-assisted pyrolysis for the generation of biochar from Dodonaea viscosa branches. *International Journal of Renewable Energy Development* 2025; 14(4): 781–793. https://doi.org/10.61435/ijred.2025.61186

[30] Tu P, Zhang G, Cen Y, Huang B, Li J, Li Y, Yuan H. Enhanced phosphate adsorption and desorption characteristics of MgO-modified biochars prepared via direct co-pyrolysis of MgO and raw materials. *Bioresources and Bioprocessing* 2023; 10(1): 49. https://doi.org/10.1186/s40643-023-00670-3

[31] Oginni O, Yakaboylu GA, Singh K, Sabolsky EM, Unal-Tosun G, Jaisi D, Shah A. Phosphorus adsorption behaviors of MgO modified biochars derived from waste woody biomass resources. *Journal of Environmental Chemical Engineering* 2020; 8(2): 103723. https://doi.org/10.1016/j.jece.2020.103723

[32] Dunuwila S, Mason JR, Teplyakov AV. Tuning physical properties and chemical reactivity of the MgO surface by chemical modification with hexafluoroacetylacetone. *Langmuir* 2025; 41(21): 12905–12913. https://doi.org/10.1021/acs.langmuir.5c00182

[33] Mahmood SS, Al-Yaqoobi AM. Production of biodiesel by using CaO nano-catalyst synthesis from mango leaves extraction. *International Journal of Renewable Energy Development* 2024; 13(6): 1025–1034. https://doi.org/10.61435/ijred.2024.60469

[34] Chabani M, Amrane A, Zermane F, Ainadjih M, Bensmaili A. Exploring the efficiency of Algerian kaolinite clay in the adsorption of chromium (Cr(III)) from industrial wastewater: Experimental and DFT insights. *Applied Sciences* 2024; 14(9): 3907. https://www.mdpi.com/1420-3049/29/9/2135

[35] Saravanan A, Senthil Kumar P, Jeevanantham S, Karishma S, Tajsabreen B, Yaashikaa PR, Reshma B. Adsorption of pollutants from wastewater by biochar: A review. *Chemosphere* 2024; 347: 140738. https://doi.org/10.1016/j.hazadv.2022.100226

[36] Akpotu SO, Farrow L, Gqoba SS, Elugoke SE, Sanusi OM, O'Regan DP, Teddy CM, Moodley R, Onyango MS. Engineered geomedia kaolin clay-reduced graphene oxide–polymer composite for the remediation of olaquindox from water. *ACS Omega* 2022; 7(38): 34054–34065. https://doi.org/10.1021/acsomega.2c03253

[37] Xu D, Gao Y, Lin Z, Gao W, Zhang H, Karnowo K, Zhang S. Application of biochar derived from pyrolysis of waste fiberboard on tetracycline adsorption in aqueous solution. *Frontiers in Chemistry* 2020; 7: 943. https://doi.org/10.3389/fchem.2019.00943

[38] Ali F, Khan MI, Iqbal M. Functionalized biochar composites for the efficient removal of emerging contaminants: A critical review. *Chemosphere* 2024; 338: 139593. https://doi.org/10.1016/j.chemosphere.2023.139593

[39] Alrefaee HA, Alsulami HB, Basfar AA. Microwave-assisted biochar modifications for enhanced contaminant adsorption: A review. *Journal of Hazardous Materials* 2023; 447: 130856. https://doi.org/10.1016/j.jhazmat.2023.130856

[40] Ali F, Muhammad M, Begum S, Ilyas M, Ali N, Khan M, AlOthman ZA. One-pot synthesis of monolith induced porous silica-graphene oxide and its application for the excellent adsorption of pinoxaden. *Microchemical Journal* 2024; 204: 111112. https://doi.org/10.1016/j.microc.2024.111112

[41] Gwenzi W, Chaukura N, Mukome FND. Modified biochars for environmental remediation: Recent progress and perspectives. *Environmental Pollution* 2023; 319: 120958. https://doi.org/10.1016/j.envpol.2022.120958

[42] Igalavithana AD, Ok YS, Mohan D. Biochar modification strategies for aqueous contaminant removal: Recent trends and future directions. *Bioresource Technology* 2022; 343: 126118. https://doi.org/10.1016/j.biortech.2021.126118

[43] Eltaweil AS, Elgarahy AM, El-Subruiti GM. Recent trends in the preparation of modified biochar and its application for pesticide removal: A review. *Journal of Environmental Chemical Engineering* 2022; 10(1): 107118. https://doi.org/10.1016/j.jece.2021.107118

[44] Ahmed MA, Alharthi MA, Hassan ME. Advances in engineered biochars for herbicide removal: Mechanisms and modeling. *Environmental Science and Pollution Research* 2024; 31(4): 5800–5815. https://doi.org/10.1007/s11356-024-29561-2

[45] Ali MA, El-Zohry AM, Al-Hosiny N. Biochar-based adsorbents for pesticide removal: Optimization and mechanistic insights. *Journal of Environmental Management* 2024; 345: 118765. https://doi.org/10.1016/j.jenvman.2023.118765

[46] Nguyen CT, Tungtakanpoung D, Kajitvichyanukul P. Kinetic, isotherm and mechanism in paraquat removal by adsorption process using corn cob biochar produced from different pyrolysis conditions. *Case Studies in Chemical and Environmental Engineering* 2022; 6: 100248. https://doi.org/10.1016/j.cscee.2022.100248

[47] Ha NTH, Toan NC, Kajitvichyanukul P. Enhanced paraquat removal from contaminated water using cell-immobilized biochar. *Clean Technologies and Environmental Policy* 2021; 23: 1–13. https://doi.org/10.1007/s10098-020-01996-8

[48] Ahmed MJ. Enhanced conversion of glycerol to glycerol carbonate on modified bio-char from reed plant. *Iraqi Journal of Chemical and Petroleum Engineering* 2019; 20(4): 15–20. https://doi.org/10.31699/IJCPE.2019.4.3

[49] Shakir SW, Hussein SS, Alzuhairi M. Optimization of CO_2 desorption from Fe_2O_3 nanofluid-based hybrid amines: A Taguchi design approach. Environmental Engineering Research. 2026 Mar 8;31(5):250716. https://doi.org/10.4491/eer.2025.716

[50] Cao Y, Jiang S, Zhang Y, Xu J, Qiu L, Wang L. Investigation into adsorption characteristics and mechanism of atrazine on nano-MgO modified fallen leaf biochar. *Journal of*

Environmental Chemical Engineering 2021; 9(4): 105727. https://doi.org/10.1016/j.jece.2021.105727

[51] Guo F, Zhou M, Xu J, Fein JB, Yu Q, Wang Y, Rong X. Glyphosate adsorption onto kaolinite and kaolinite-humic acid composites: Experimental and molecular dynamics studies. *Chemosphere* 2021; 263: 127979. https://doi.org/10.1016/j.chemosphere.2020.127979

[52] Hussein SS, Al-Yaqoobi AM, Shakir SW, Al-Naseri HA, Ahmed AM, Al-Dahhan M. Enhanced Carbon Dioxide (CO_2) Absorption using Fe_2O_3-Loaded MEA/TEA Nanofluids: A Statistical and Experimental Study. *Journal of Advanced Research in Fluid Mechanics and Thermal Sciences* 2025; 129(2): 133–149. https://doi.org/10.37934/arfmts.129.2.133149

[53] Alrefaee SH, Aljohani M, Alkhamis K, Shaaban F, El-Desouky MG, El-Bindary AA, El-Bindary MA. Adsorption and effective removal of organophosphorus pesticides from aqueous solution via novel metal-organic framework: Adsorption isotherms, kinetics, and optimization via Box-Behnken design. *Journal of Molecular Liquids* 2023; 384: 122206. https://doi.org/10.3390/molecules29184317